Research Highlights

DOI: 10.1039/b510683b

Radial temperature gradients for PCR

Over the past decade a variety of microfabricated devices for performing DNA amplification have been reported. Development of such technology has been driven by the significant performance gains that accompany system downsizing. In simple terms, the key to these performance gains lies in improved thermal and mass transfer on a small scale. Heat can be transferred to and removed from microfluidic reaction environments exceptionally quickly and system temperatures can be controlled uniformly throughout the sample volume. Not surprisingly, microfluidic systems have been successful in enabling high-efficiency and ultra-fast DNA amplification. The normal approach to instrument miniaturization involves the direct downsizing of system dimensions to reduce thermal masses. An alternative approach utilises a flow-based system where, instead of heating and cooling a static sample to effect PCR, the sample is moved between reaction zones held at specific temperatures. Originally described by Kopp *et al.*,[1] continuous-flow PCR allows ultra-fast reaction times, since the small-volume fluid elements can be heated or cooled to the required temperature within 100 milliseconds. Although continuous-flow PCR allows high-throughput processing of multiple samples, the fixed configuration of the fluidic channel pattern is somewhat restrictive in terms of configurational flexibility (for example the number of cycles is essentially defined by the microdevice structure). To address this limitation, some researchers have utilized a 'reagent shunting' scheme, whereby reagents are moved backwards and forwards between regions held at a constant (and varying) temperature. Indeed, Ji-Yen Cheng and colleagues at the Research Center for Applied Sciences in Taiwan have recently described a novel thermal cycling strategy for performing shunted PCR within microchannel environments.[2]

The most interesting aspect of this work involves the generation and use of a radial temperature gradient for thermal cycling (rather than using a number of discrete temperature zones). Specifically, the authors fabricate a circular microfluidic device in PMMA. The fluidic channel (1.2 mm wide, 0.6 mm deep and 70 mm long) within this consists of three interconnected arcs (Fig. 1) which are used for denaturing, annealing and extension. To effect thermal cycling this structure is contacted with the heater chip (fabricated from ITO-coated glass) that contains both an inner and outer heating ring (Fig. 1). These rings are connected by ITO strips, and through selective application of a voltage to these strips the temperature of each ring can be controlled. Depending on the relative position of the high-power and low-power heating rings two different kinds of radial temperature gradient can be generated. In the first (when the high-power ring is near the chip centre) a cone-shaped distribution results, in which temperature decreases as a function of distance away from the centre, and in the second (when the high-power ring is positioned near the chip edge) an annular type distribution results with temperature minimizing at the chip centre. Importantly, both distributions are radially symmetric, and thus precise control of the temperature within each fluidic arc can be achieved through variation of the applied voltage and thus the gradient characteristics. In assessing both surface and microchannel temperatures using non-contact IR thermometry and spectral analysis of thermochromic liquid crystals, the authors find that temperature gradients of approximately 2 °C mm^{-1} are achieved in the current system. Significantly this approach successfully generates large temperature gradients without the need for active temperature control or thermal isolation of temperature zones.

When using the system to perform PCR, microchannel walls are coated with amorphous Teflon to reduce surface energy and ensure that the liquid samples form a unified plug when pumped through the channel. Injection of compressed air is then used to manoeuvre liquid plugs within the microchannel and sample shuttling between desired temperature locations is achieved by varying the applied pressure. Each cycle of a 23-cycle PCR involves retaining a 4.5 μL sample in the denaturing arc (95 °C) for 180 s, pumping it to the annealing arc (57 °C) and holding it there for 30 s, pumping it to the extension arc (72 °C) and incubating for 30 s, and finally sending the plug back to the denaturing arc and incubating for 30 s. In this way a 23-cycle amplification takes approximately 38 min and yields the expected product (analysed by slab-gel electrophoresis). The studies presented describe a nice modification to flow-based reactors for PCR due to the high-levels of thermal control and the ability to vary cycle numbers in a trivial fashion.

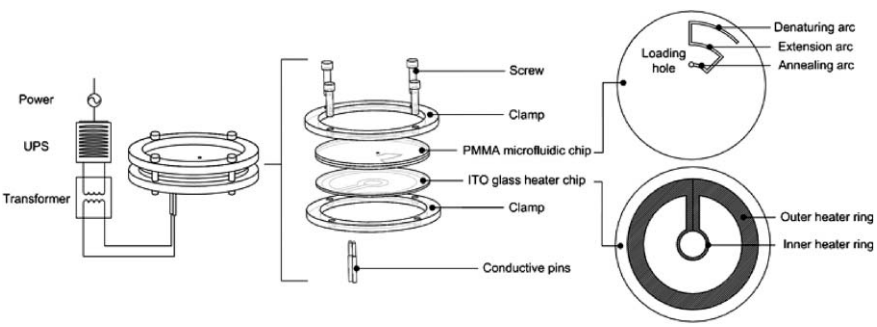

Fig. 1 Microfluidic PCR reactor. The microfluidic and heater chips are clamped together. All components other than the glass chip and the conductive pins are made of plastic. The heater chip is fabricated from ITO-coated glass. The shaded area denotes the energized strips used for heating. The microfluidic chip is fabricated from PMMA.

Indeed, the authors expect that the chip system will be ideally suited to other processing operations in which thermal control is important.

Microfluidic capsule formation

In recent times the manipulation of immiscible fluids within microfluidic environments has been exploited in a wide variety of analytical and synthetic applications. At the heart of these developments are the dramatically different flow characteristics of immiscible fluids when compared to miscible liquid streams. Using relatively simple fluidic systems and flow control architectures particles, droplets, and emulsions may be formed at high speeds and with controllable characteristics (such as size, size distribution and chemical composition). A number of reports have described how such systems may be used to create solid particles and hollow capsules. In all these studies a two-step procedure, combining droplet formation and downstream polymerisation, has been employed. Although elegant and successful in their application such microfluidic systems can be complex to fabricate. To this end, Tyler McQuade and co-workers at Cornell University have recently reported a rather different and simple approach to capsule formation that relies on interfacial polymerisation as the droplet forms.[3] Moreover, the microfluidic system described is made from common laboratory tubing and syringe needles, thus allowing rapid construction and reconfiguration.

In initial studies the authors generate organic droplets by introducing an organic solution through a 30 gauge needle inserted through the wall of 1.6 mm internal diameter PVC tubing containing a continuous aqueous phase. As can be seen in Fig. 2, this

Fig. 2 Photograph of fluidic device including needle and dye-filled organic droplets dispersed in the continuous aqueous phase. (Adapted with permission. Copyright 2005, The American Chemical Society.)

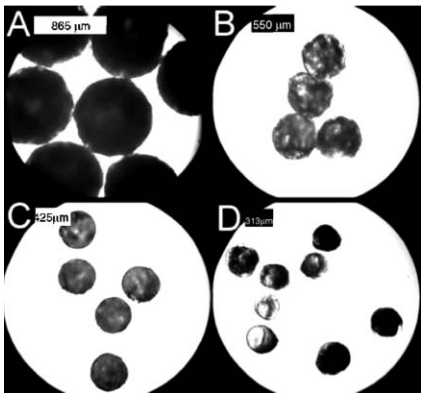

Fig. 3 Light microscope images of capsules in water formed with constant organic flow rate (0.141 mL min^{-1}) and increasing aqueous flow rate: (A) 2.00 mL min^{-1}; (B) 11.0 mL min^{-1}; (C) 13 mL min^{-1}; (D) 25 mL min^{-1}. (Adapted with permission. Copyright 2005, The American Chemical Society.)

configuration results in similar behaviour to that observed in planar microfluidic devices. Studies then focus on interfacial polymerisation of the monodisperse flow phase to form a polyamide shell. Specifically, polyethyleneimine present in the aqueous stream and a mixture of sebacoyl and trimesoyl chloride in the dispersed phase are contacted at the needle/tube interface and result in oil-filled polyamide capsules. Fig. 3 shows that these capsules are monodisperse with an average size that is dependent on the relative flow rates of the input flow streams. The authors expect that smaller capsules may be formed by using narrower gauge needles and are currently investigating the synthesis of anisotropic particles in similar devices. Overall, the studies presented are of particular merit due to the simplicity of the system fabrication and operation, and most importantly the ability to naturally initiate coaxial confinement of the dispersed phase.

Protein crystal nucleation in droplets

The ability to control nucleation of protein crystals is enabling in various fields, including protein crystallography, production of protein crystalline pharmaceuticals, protein separation, and the treatment of protein condensation diseases. For example, the determination of the three-dimensional structures of proteins by crystallographic techniques remains a time-consuming process. One reason for this is the difficulty of growing protein crystals of adequate quality for analysis. Many studies have suggested that the success of protein crystallization depends sensitively on the physical conditions of the initial solution environment, and it is therefore critical to understand the physical factors that determine whether a given solution will produce good crystals. To date, few if any studies have assessed the role that mixing has on the nucleation of protein crystals. This has been largely due to the difficulties associated with controlling and monitoring mixing processes in batch systems. To address this important issue Rustem Ismagilov and associates at the University of Chicago have recently used a plug-based microfluidic reactor to monitor mixing phenomena and their influence on protein crystal nucleation.[4] Importantly, the approach allows hundreds of individual experiments to be performed in short times and requires minimal volumes of reagent. The authors generate a train of nL aqueous plugs within a continuous immiscible carrier fluid which act as discrete reaction vessels. In the current experiments three inlets containing buffer, protein and salt feed the aqueous stream. To alter mixing, the overall flow rate is varied whilst maintaining the flow rate ratio between buffer, salt and protein. Mixed plugs are then collected in a capillary, incubated at a fixed temperature and monitored for protein crystallization.

Using this general approach the authors confirm the dependence of nucleation on flow rate and mixing. Specifically, studies demonstrate that nucleation is enhanced at low flow velocities, and hindered at high flow velocities (Fig. 4). Through an appreciation of mixing by chaotic advection, this behaviour is expected since the number of nucleation events depends on both interfacial areas and interface lifetimes. Other studies include an assessment of channel geometries. These are significant since plugs moving through straight channels do not mix chaotically, which means that interfacial areas are reduced and less nucleation events expected. In addition, variations in flow velocity within straight channels should not appreciably affect mixing (unlike similar

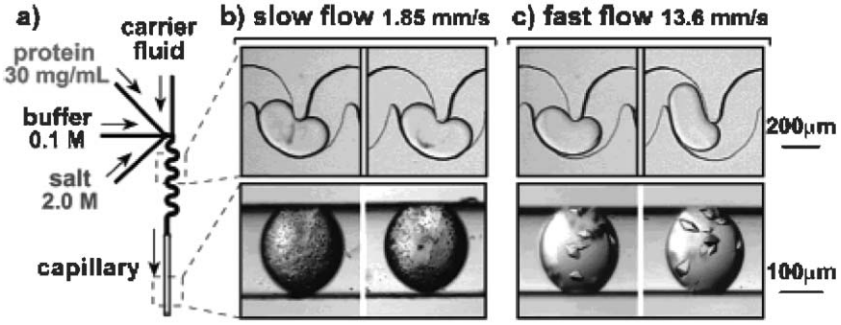

Fig. 4 A schematic of the microfluidic plug reactor. (b) At low flow velocities precipitation occurs and microcrystals grow. (c) At high flow velocities no precipitation occurs and large crystals grow. (Adapted with permission. Copyright 2005, The American Chemical Society.)

variations in winding channels). Experiments confirm both these predictions and further confirm the general features of mixing and nucleation within the microfluidic system. In general, the presented studies demonstrate that nucleation rates are dependent on the area and lifetime of solution interfaces, rather than the just the mixing time. Such information will undoubtedly prove useful in precise control of nucleation events in a variety of chemical and biological systems.

Microchemostat for bacterial monitoring

Microbial biofilms pose challenges in continuously operating bioreactors. They interfere with bioreactor operation and shed their progeny into bulk cultures to create impure mixed cultures. Although there are numerous potential advantages associated with fabricating microscale bioreactors (including reduced reagent and growth media volumes), these wall-growth effects are aggravated due to the dramatic increase in the surface area-to-volume ratio within such environments. To address this issue, Stephen Quake and colleagues at the California Institute of Technology have recently reported the fabrication and testing of a chip-based bioreactor that actively prevents biofilm formation and allows semi-continuous planktonic growth in independent nL reactors.[5] Furthermore optical measurements allow cultures monitoring and provide for automated, real-time, and non-invasive assessment of cell density and morphology with single cell resolution.

Each reactor consists of a growth chamber, an integrated peristaltic pump and valves to control reagent addition, waste removal and cell collection (Fig. 5). These 'microchemostats' function in two alternating states. In the first, the peristaltic pump motivates the culture medium around a growth loop at a constant linear velocity. In the second, circulation is stopped, and a segment of the growth medium is removed. This portion is then flushed with a lysis buffer to remove cells, flushed with sterile growth medium to remove excess lysis buffer and then recombined with the rest of the growth chamber fluid. Repetition of this process allows semi-continuous reactor operation whilst preventing significant biofilm formation.

The authors demonstrate that this active removal of wall-adhering cells is considerably more effective than passive

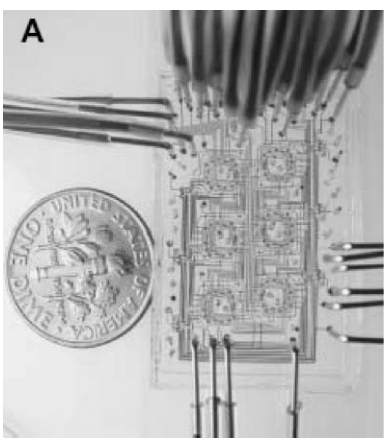

Fig. 5 Optical micrograph of six microchemostats integrated on a single planar chip. (Adapted with permission. Copyright 2005, American Association for the Advancement of Science).

treatments involving non-adhesive surfaces coatings (where fluidic channels are invaded by biofilms within a period of 48 hours). The performance of the microchemostat was demonstrated in over 40 growth experiments with *E. Coli* MG1655 cells using a variety of growth conditions. Under typical conditions, bacterial growth commenced after a lag period and consisted of exponential growth followed by steady-state saturation. Steady-state cell concentrations scaled with dilution rates and nutrient richness. The microchemostats were also used to successfully monitor dynamics of cell populations containing a synthetic "population control" circuit. Significantly, such an arrangement allows autonomous regulation of cell density through modulation of the expression of a killer gene (which controls cell death rate).

Through detailed studies of cell growth and death, the authors demonstrate that such microfluidic circuits are more stable than in macroscale cultures (under similar growth conditions) where regulation of cells is lost within 48–70 hours. In the microchemostat systems studies, cell regulation was sustained for more than 200 hours and in some cases in excess of 500 hours.

The microchemostats described have a working volume of 16 nL, actively suppress biofilm formation and allow automated culturing and monitoring of cell growth in populations of between 100 and 10000 bacteria. In addition, the authors expect that further reductions in reactor volume will suppress the total mutation rate and extend monitoring of genetically homogenous populations. Such capabilities should find useful applications in high-throughput screening methods used in chemical genetics and pharmaceutical discovery.

Rapid prototyping of nanofluidic devices

Current approaches for the creation of three-dimensional microfluidic networks often involve the use of experimentally complex fabrication protocols. For example, the simplest route to multilayer structures involves alignment and subsequent stacking of prefabricated two-dimensional structures. Although successful such methods are

time-consuming, rely on precise alignment between fluidic layers and are only applicable to relatively simple networks. Soft-lithographic techniques have to some extent allowed more direct routes to the fabrication of complex, multilayer fluidic structures; however these techniques are typically confined to relatively thin device architectures and constrained by limited substrate materials. A brief survey of the recent literature illustrates that the most common routes towards the creation of complex, three-dimensional microfluidic networks involve the processing of polymeric or plastic materials. Such materials are often ill-suited to applications involving the use of organic solvents and high-pressures. Glasses possess beneficial properties such as well-defined surface chemistries, superior optical characteristics and good electroosmotic properties. However, machining these materials to create complex, three dimensional fluidic structures has traditionally presented a number of problematic issues that have hindered widespread application.

To address this limitation, Alan Hunt and colleagues at the University of Michigan, Ann Abor have demonstrated direct 3D-machining of submicron diameter, fluidic channels in glass.[6] The approach involves removing glass from the substrate by inducing optical breakdown with a focused femtosecond pulsed laser. Importantly, machining is direct and can create both long and deep channels with excellent surface characteristics. Furthermore, if machining is performed under a fluid, microbubbles produced at the site of optical breakdown gently force debris away from the machining site.

The authors illustrate the efficacy of their approach by fabricating a number of key components utilised in three-dimensional fluidic networks. In all cases, machining is performed using a diode-pumped Nd:glass laser that is frequency doubled to generate 800 fs pulses, of 10–20 nJ pulse^{-1} at 527 nm.

A nice application of the power of the machining technique is in the construction of out-of-plane jumpers that allow fluid streams to cross paths without mixing. The concept is shown schematically in Fig. 6(a), with an SEM image of the jumper cross section shown in Fig. 6(b). The jumper is generated in less than three minutes and has excellent surface roughness. Moreover, the authors show that long channels can be fabricated in small areas for use in chromatographic separations. Finally, the ability to create 3D geometries allows fabrication of efficient mixing structures. Specifically, structures are fabricated where two different input streams are divided into four streams that form an interdigitated mixing arrangement (through use of jumper structures). As is well-known, this arrangement increases contact interfaces and reduces diffusion lengths, thus allowing rapid mixing in a low Reynolds number regime. The development of such a rapid and versatile machining tool is likely to prove useful in creating a diversity of highly integrated microfluidic devices in a range of rigid materials with short prototyping times.

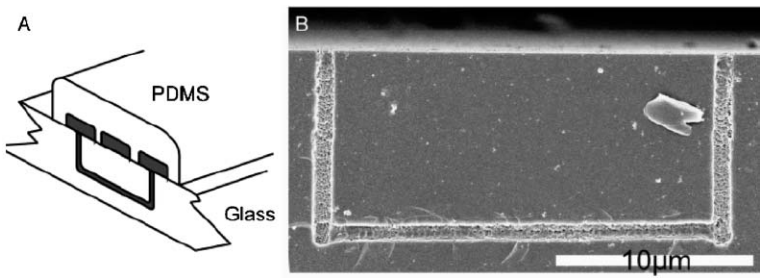

Fig. 6 (a) Schematic of 'nanojumper' that joins two streams separated by a middle steam without mixing. (b) SEM of a cross section of the nanojumper. (Adapted with permission. Copyright 2005, The American Chemical Society.)

Nanofluidic filters for protein concentration

The small sample volumes usually encountered in microfluidic environments (pL–nL) dictate that efficient detection has become a key issue in defining the applicability of many microfluidic systems to biological problems. Although a diversity of high-sensitivity optical and electrochemical techniques have been used to interrogate small volume analytical systems, on-line sample concentration methods are often required in applications where the target analyte is present at very low concentration. A good example of this situation is in proteome analysis. Very simply, proteomics is an immense challenge due to the sheer number of proteins present in most biological samples. Up to 50,000 proteins may be simultaneously present in a eukaryotic cell, and due to the large dynamic range of protein expression these proteins will exist in vastly differing quantities and concentrations. Consequently, only a small fraction of all proteins present in the sample are typically open for analysis.

A range of strategies for sample pre-concentration in liquids have been developed in macroscale systems and transferred to chip-based formats. Such methods have enabled in-line pre-concentration in excess of three orders of magnitude. Recently, Jongyoon Han and co-workers at Massachusetts Institute of Technology have developed a novel and highly efficient approach for microfluidic sample pre-concentration based on electrokinetic trapping and nonlinear electroosmotic flow.[7] The device is fabricated using standard photolithography and etching techniques and importantly does not require specialised reagents or membrane materials. Nanofluidic channels typically between 30 and 70 nm deep are used to connect two microfluidic channels 10 to 20 μm wide and 1.5 μm deep. An electric field generated in the nanofluidic filter is used to generate an ion-depletion region and an extended space-charge layer which can trap biomolecules, whilst a tangential electric field in the microchannel (on the anodic side) is used to generate an electroosmotic flow to drive molecules into the trap.

Testing of the device demonstrates rapid pre-concentration of proteins and peptides within microfluidic channels, without any physical barrier, and pre-concentration factors of 10^6–10^8. Furthermore, coating channel surfaces with polyacrylamide eliminates protein

adsorption and affords better control of surface charge densities. Finally, the authors also report successful coupling of the pre-concentrator with downstream zone electrophoresis of collected proteins. Overall, the combination of such a microfluidic pre-concentration unit with biomolecule discrimination offers an attractive platform for integrated biomarker detection, environmental analyses and chemical–biological agent detection. Importantly, such systems can also be applied to the analysis of complex protein mixtures without sacrificing detectability of minor components.

Andrew J. de Mello

References

1 M. U. Kopp, A. J. de Mello and A. Manz, *Science*, 1998, **280**, 1046.

2 Ji-Yen Cheng, Chien-Ju Hsieh, Yung-Chuan Chuang and Jing-Ru Hsieh, *Analyst*, 2005, **130**, 931–940.

3 E. Quevedo, J. Steinbacher and D. T. McQuade, *J. Am. Chem. Soc.*, 2005, **127**, 10498–10499.

4 D. L. Chen, C. J. Gerdts and R. F. Ismagilov, *J. Am. Chem. Soc.*, 2005, **127**, 9672–9673.

5 Frederick K. Balagaddé, Lingchong You, Carl L. Hansen, Frances H. Arnold and Stephen R. Quake, *Science*, 2005, **309**, 137–140.

6 Kevin Ke, Ernest F. Hasselbrink, Jr. and A. J. Hunt, *Anal. Chem.*, 2005, **77**, ASAP article, DOI: 10.1021/ac0505167.

7 Ying-Chih Wang, Anna L. Stevens and Jongyoon Han, *Anal. Chem.*, 2005, **77**, 4293–4299.